

Investigation of interface spacing, stability, band offsets and electronic properties on (001) SrHfO₃/GaAs interface : First principles calculations

Li-Bin Shi,^{1, a)} Xiao-Ming Xiu,¹ Xu-Yang Liu,¹ Kai-Cheng Zhang,¹ Chun-Ran Li,¹ and Hai-Kuan Dong^{1, b)}
School of Mathematics and Physics, Bohai University, Liaoning Jinzhou 121013, China

(Dated: 8 March 2024)

SrHfO₃ is a potential dielectric material for metal-oxide-semiconductor (MOS) devices. SrHfO₃/GaAs interface has attracted attention due to its unique properties. In this paper, the interface properties of (001) SrHfO₃/GaAs are investigated by first principles calculations based on density functional theory (DFT). First of all, the adsorption behavior of Sr, Hf and O on GaAs surface is investigated. O has lower adsorption energy on Ga surface than on As surface. Then, some possible (0 0 1) SrHfO₃/GaAs configurations are considered to analyze the interface spacing, stability, band offsets and charge transfer. HfO₂/Ga(2) and SrO/Ga(1) configurations in binding energy are lower than other interface configurations, indicating that they are more stable. At last, we study the electronic properties of HfO₂/Ga(2) and SrO/Ga(1) configurations. The electronic density of states suggests that the systems exhibit metallic behavior. The band offset and charge transfer are related to the interface spacing. The valence band offset (VBO) and charge transfer will decrease with increasing interface spacing.

PACS numbers: 68.35.-p, 71.15.Mb, 77.55.D-

I. INTRODUCTION

In order to reduce the feature size of metal-oxide-semiconductor-field-effect-transistors (MOSFETs), we have to replace traditional silicon dioxide gate dielectric with high permittivity (high- κ) materials.^{1,2} A lot of research has been done on high- κ dielectrics, including Si₃N₄,³ Ge₃N₄,⁴ Gd₂O₃,⁵ La₂O₃,⁶ Y₂O₃,⁷ Al₂O₃,⁸ ZrO₂,⁹ HfO₂,¹⁰ SrTiO₃,¹¹ and SrHfO₃.¹²⁻¹⁵ Among them, SrHfO₃ becomes a promising candidate because of its good current voltage characteristics, large band offsets, high dielectric constant, and low frequency dispersion. GaAs-based MOSFETs exhibit promising performance due to its higher electron velocity.¹⁶ It is found that single crystal interface usually exhibits excellent properties. For example, single crystal Gd₂O₃/GaAs interface exhibits very low leakage current density with the value from 10⁻⁹ A/cm² to 10⁻¹⁰ A/cm².⁵ Cubic SrHfO₃ has a experimental lattice constant of 4.07 Å, which is approximately equal to 4.00 Å in-plane spacing of GaAs.¹⁷ This provides convenient conditions for the production of single crystal SrHfO₃/GaAs interface.

At present, some theoretical and experimental studies have been done on SrHfO₃.¹⁷⁻²¹ Mcdaniel et al.¹⁷ successfully deposited crystalline SrHfO₃ films on Ge substrates. It is found that valence band offset (VBO) and conduction band offset (CBO) are 3.27 eV and 2.17 eV, respectively. Sousa et al.¹⁸ successfully deposited epitaxial SrHfO₃ films on Si substrates. A band gap of 6.1 eV was measured optically. Sawkar-Mathur et al.¹⁹ successfully prepared SrHfO₃ films on Si. The SrHfO₃ exhibited a lattice mismatch of 6% with silicon. Wang et al.²¹ stud-

ied the electronic and structural properties of SrHfO₃ by first principles calculations. The adsorption of Ga and As on SrO and HfO₂ surfaces is systematically investigated. It is found that Ga and As preferentially adsorb at the top of O. In practice, the oxide is usually deposited on semiconductor substrate.^{18,22,23} It is more realistic to study the adsorption behaviors of Sr, Hf and O on GaAs surface. The adsorption behaviors of these atoms can provide useful information for determining interface stability. However, we still do not find a detailed theoretical or experimental study for SrHfO₃ growth on GaAs.

In this study, we investigate the growth of SrHfO₃ on GaAs. The adsorption behaviors of Sr, Hf and O on GaAs surface are studied. We deeply understand the stability of SrHfO₃/GaAs by calculating binding energy. Band alignment between SrHfO₃ and GaAs is investigated. The interface behaviors are analyzed by charge transfer and electronic density of states.

II. COMPUTATIONAL DETAILS

The calculations on structural and electronic properties of SrHfO₃ and GaAs are performed using the CASTEP code, which is based on density functional theory and plane-wave pseudopotential method. Local density approximation (LDA) is chosen as exchange correlation functional. The valence electron configurations for Sr, Hf, Ga, As and O are considered as 4s²4p⁶5s², 5d²6s², 3d¹⁰4s²4p¹, 4s²4p³ and 2s²2p⁴, respectively. The cores are represented by norm-conserving pseudopotential, while the valences states are expanded in a plane-wave basis set with energy cutoff of 600 eV. The 6×6×6 k point sampling is used for SrHfO₃ and GaAs calculations, which is generated by the Monkhorst-Pack scheme.²⁴ The crystal structures of SrHfO₃ and GaAs are shown

^{a)}Electronic mail: slb0813@126.com; shilibin@bhu.edu

^{b)}Electronic mail: bhk@bhu.edu.cn

in Fig. 1. The geometry optimization will finish if the maximum force on each atom is less than 0.01 eV/Å. The calculated lattice constant for SrHfO₃ is 4.02 Å, which is in agreement with theoretical value of 4.16 Å²⁰ and experimental value of 4.07 Å.¹⁷ It is a little larger than in-plane spacing of GaAs with the value of 3.94 Å. The lattice mismatch between SrHfO₃ and GaAs is estimated to be 2.0%, which is agreement with the reported value of 1.8%.²¹ The band gaps calculated by LDA functional are $E_g^{\text{GaAs(LDA)}}=0.78$ eV and $E_g^{\text{SrHfO}_3\text{(LDA)}}=3.60$ eV. We attempt to improve the band gaps using hybrid Heyd-Scuseria-Ernzerhof functional (HSE).^{25–29} The values calculated by HSE functional are $E_g^{\text{GaAs(HSE)}}=1.58$ eV and $E_g^{\text{SrHfO}_3\text{(HSE)}}=5.37$ eV, which are close to experimental values of $E_g^{\text{GaAs}}=1.42$ eV^{16,30} and $E_g^{\text{SrHfO}_3}=6.01$ eV.¹⁷

In order to investigate interface properties of (001) SrHfO₃/GaAs, we construct 2×2 surface supercell. Because SrHfO₃ is usually grown on GaAs substrates, the lattice constants of the interface are determined by those of GaAs. The interface consists of 11-layer SrHfO₃ and 17-layer GaAs. A vacuum region of 15 Å is used to avoid the interaction between the top and bottom layers. GaAs slab consists of alternating layers of Ga and As, while SrHfO₃ slab consists of alternating layers of SrO and HfO₂. In order to avoid polarization effect, SrHfO₃ and GaAs are modeled using a symmetric slab.^{11,21} Ten kinds of interface configurations are considered to calculate, which is shown in Fig. 2. These configurations involve in depositing SrO or HfO₂ layers on Ga or As surface. The atom located at the center of four Ga or As is called as fourfold hollow site. The atom located between two Ga or As is called as bridge site. For HfO₂/Ga(1) interface, 4 Hf are located on the top of Ga, and 8 O at the bridge site. For HfO₂/Ga(2) interface, 4 O are located on the top of the Ga, 4 O at the fourfold hollow site, and 4 Hf at the bridge site. For HfO₂/Ga(3) interface, 8 O are located at the bridge site, and the 4 Hf at the fourfold hollow site. For SrO/Ga(1) interface, 4 O are located on the top of Ga, and 4 Sr at the fourfold hollow site. For SrO/Ga(2) interface, O and Sr are located at the bridge site. It is well known that the LDA functional underestimates the band gap of semiconductors and insulators. Therefore, the nonlocal functional is usually used to investigate the band gap.²⁹ However, the adsorption energy and binding energy only consider the system energy difference, so the result calculated by the LDA functional is reliable.^{31,32}

The parameters for the interface calculation are different from those for the bulk calculation. $2 \times 2 \times 1$ k-points are used for integrations over the Brillouin zone. In the geometry relaxations, the atoms near interface and vacuum region are allowed to relax. The polarization inside SrHfO₃ and GaAs slabs does not affect the atomic relaxation.

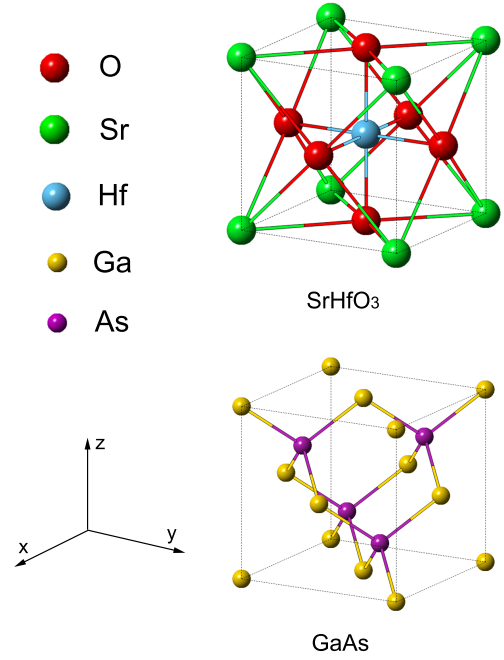


FIG. 1. Crystal structure of SrHfO₃ and GaAs. The coordinate axis is marked in the graph.

TABLE I. The adsorption energy per atom in units of electron volt(eV). T, B, and H denote top, bridge, and hollow sites, respectively.

Adsorption position	O adatom	Sr adatom	Hf adatom
T_{Ga}	-7.24		-4.00
B_{Ga}	-8.37	-3.29	-5.72
H_{Ga}	-7.34	-4.45	-9.21
T_{As}	-6.51		-3.94
B_{As}	-7.17	-4.31	-6.72
H_{As}	-4.67	-5.46	-8.70

III. RESULTS AND DISCUSSION

A. The (001) SrHfO₃/GaAs interface

Firstly, we study the adsorption behaviors of O, Sr and Hf on (001) GaAs slab. The (001) GaAs slab has a vacuum region of 15 Å. The adsorption atom is gradually close to the absorption site. Adsorption energy is defined as the following expression:³³

$$E_{\text{ads}} = E(\text{GaAs} + \text{ads}) - E(\text{GaAs}) - E(\text{ads}) \quad (1)$$

where $E(\text{GaAs}+\text{ads})$ is the total energy of a adsorption system with adatom, $E(\text{GaAs})$ is the total energy of the clean (001) GaAs slab, and $E(\text{ads})$ is the energy of adatom. We examine these adatoms at the fourfold

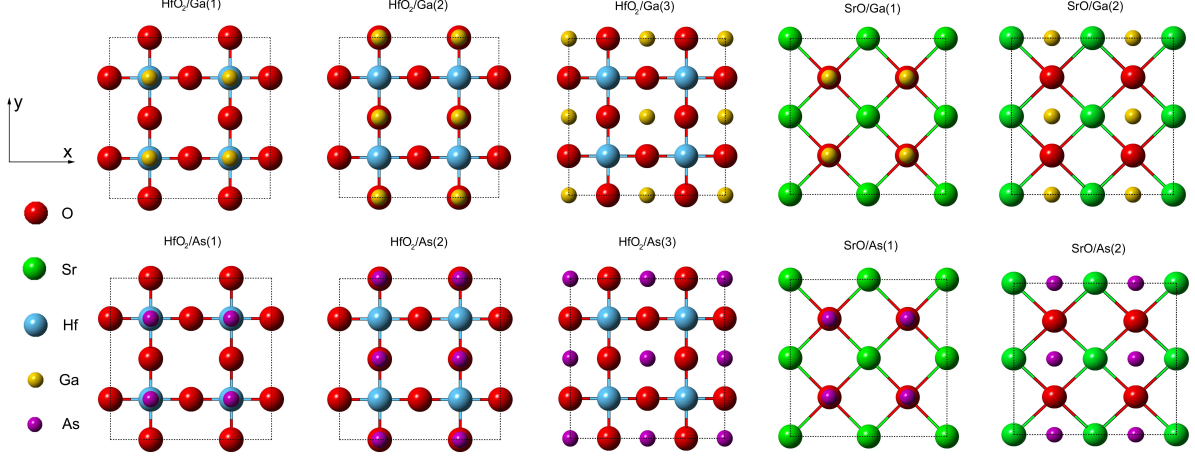


FIG. 2. The schematic of the (001) $\text{SrHfO}_3/\text{GaAs}$ interfaces. We assume that (001) SrHfO_3 is deposited onto (001) GaAs substrate. 10 kinds of possible interface configurations are displayed. In order to facilitate the observation, we only give the atomic distribution at the interface.

TABLE II. Optimized interface spacing, binding energy, band offsets (VBO and CBO), interface atom migration, and charge transfer. The value in parentheses is the interface spacing without atom relaxation.

Interface	Interface spacing (Å)	Binding energy ($\text{eV}/\text{\AA}^2$)	VBO (eV)	CBO (eV)	O(Å)	Hf(Å)	Sr(Å)	Ga(Å)	As(Å)	Charge (e)
$\text{HfO}_2/\text{Ga}(1)$	2.8(2.9)	-0.024	2.89	1.70	0.44, -0.42	-0.01		0.07		-0.70
$\text{HfO}_2/\text{Ga}(2)$	2.2(2.1)	-0.038	4.40	0.19	0.28, -0.47	-0.07		-0.06		-1.08
$\text{HfO}_2/\text{Ga}(3)$	2.3(2.3)	-0.017	3.57	1.02	0.39, -0.47	-0.03		-0.07		-0.72
$\text{SrO}/\text{Ga}(1)$	1.7(1.9)	-0.048	4.38	0.21	-0.02		-0.14	-0.19		-0.40
$\text{SrO}/\text{Ga}(2)$	2.4(2.5)	-0.017	2.91	1.68	-0.02		-0.203	0.07		-0.08
$\text{HfO}_2/\text{As}(1)$	2.9(2.9)	-0.034	2.50	2.09	-0.31	0.04			-0.07	-0.24
$\text{HfO}_2/\text{As}(2)$	2.5(2.9)	-0.017	2.81	1.78	0.41	-0.02			-0.03	-0.60
$\text{HfO}_2/\text{As}(3)$	2.8(2.8)	-0.010	3.04	1.55	0.38	-0.05			-0.08	-0.32
$\text{SrO}/\text{As}(1)$	2.9(2.6)	-0.008	2.12	2.76	-0.03		-0.18		-0.02	0.17
$\text{SrO}/\text{As}(2)$	2.8(2.8)	-0.009	1.92	2.67	-0.04		-0.18		-0.04	0.20

hollow site, bridge site, and top site of Ga or As. Table 1 presents the calculated results. For Ga surface, Sr and Hf preferentially adsorb at Ga fourfold hollow site, while O preferentially adsorb at Ga bridge site. Similar results can also be found on As surface. It is noted that adsorption energy of O atom is lower on Ga surface than on As surface, which is in agreement with previous investigation.³⁴ Previously, Wang et al.²¹ investigated the adsorption behavior of Ga and As on SrO and HfO_2 surface. They found that Ga and As preferentially adsorb at the top of O, and As is more favorable in energy than Ga. We investigate the growth behavior of SrHfO_3 deposited on GaAs substrate, while they analyze the growth behavior of GaAs deposited on SrHfO_3 substrate. This difference is mainly due to different film growth mechanisms.^{35,36}

In order to investigate the stability of (001)

$\text{SrHfO}_3/\text{GaAs}$ interface, we also calculate the interface binding energy, which is defined as³⁷

$$E_b(\text{SrHfO}_3/\text{GaAs}) = [E_i(\text{SrHfO}_3/\text{GaAs}) - E_s(\text{SrHfO}_3) - E_s(\text{GaAs})]/2S \quad (2)$$

where $E_i(\text{SrHfO}_3/\text{GaAs})$ is total energy of $\text{SrHfO}_3/\text{GaAs}$ interface, $E_s(\text{SrHfO}_3)$ and $E_s(\text{GaAs})$ denote total energy of SrHfO_3 and GaAs surface, respectively, S is the cross-sectional area of the interface, and the factor 2 denotes two identical interfaces in the supercell. In this study, we accurately determine the interface spacing by two steps. We first roughly estimate the interface spacing by total energy calculation. We do not allow the atoms to relax, only calculate the total energy of the system at different interface spacing. The interface spacing is changed in the range from 1 Å to 5 Å with the interval

of 0.1 Å. Figure 3 presents binding energy versus interface spacing. Although the symmetrical slab is adopted in the calculation, the binding energy curves can still reflect the binding characteristics of different interfaces. The lowest binding energy and interface spacing are -0.022 eV/Å² and 2.9 Å for HfO₂/Ga(1), -0.031 eV/Å² and 2.1 Å for HfO₂/Ga(2), -0.015 eV/Å² and 2.3 Å for HfO₂/Ga(3), -0.049 eV/Å² and 1.9 Å for SrO/Ga(1), -0.019 eV/Å² and 2.5 Å for SrO/Ga(2), -0.019 eV/Å² and 2.9 Å for HfO₂/As(1), -0.011 eV/Å² and 2.9 Å for HfO₂/As(2), -0.008 eV/Å² and 2.8 Å for HfO₂/As(3), -0.012 eV/Å² and 2.6 Å for SrO/As(1), -0.012 eV/Å² and 2.8 Å for SrO/As(2). The negative binding energy indicates that the interface is stable. It is found that the binding energies for HfO₂/Ga(2) and SrO/Ga(1) are lower than those for other interface configurations, which suggests that HfO₂/Ga(2) and SrO/Ga(1) interfaces are more stable. The binding energy curve of HfO₂/As(2) interface exhibits abnormal peak, which is independent of the chosen exchange correlation functional and neglecting spin polarization. This abnormal behavior may be due to the competition between Hf-As and O-As interactions. The binding energy is -0.325 eV/Å² for CoO/MnO interface³⁸, -0.033 eV/Å² for Cu₂ZnSnS₄/ZnO interface³⁹, and -0.315 eV/Å² for Mg/Al₄C₃ interface.⁴⁰

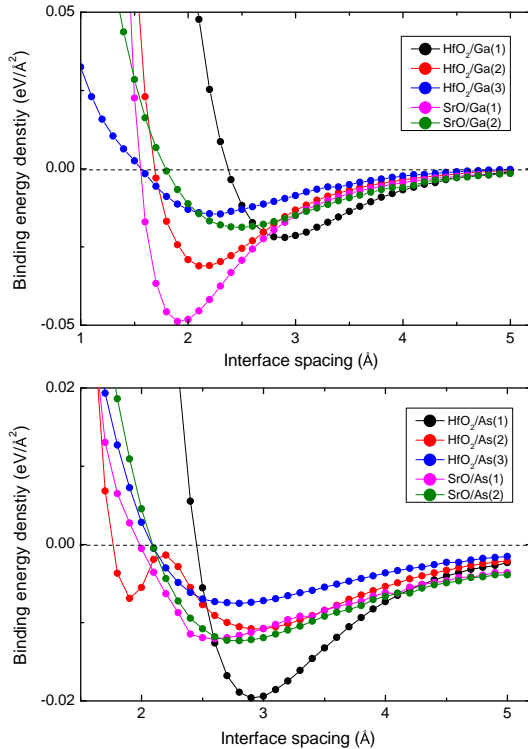


FIG. 3. Binding energy versus interface spacing for ten kinds of possible interface configurations.

In order to accurately determine the interface spacing, we allow the atoms near interface and vacuum re-

gion to fully relax. The system has the lowest energy at the optimized interface spacing. Therefore, interface spacing is determined by the lowest energy. The value is 2.8 Å for HfO₂/Ga(1), 2.2 Å for HfO₂/Ga(2), 2.3 Å for HfO₂/Ga(3), 1.7 Å for SrO/Ga(1), 2.4 Å for SrO/Ga(2), 2.9 Å for HfO₂/As(1), 2.5 Å for HfO₂/As(2), 2.8 Å for HfO₂/As(3), 2.9 Å for SrO/As(1), and 2.8 Å for SrO/As(2). Table 2 gives the binding energy, band offsets, atom migration, and charge transfer under optimized interface spacing. The values in parentheses are the interface spacing without atom relaxation. Some of the interface spacings slightly change after atom relaxation. The interface spacing for stable heterojunction is normally in the range of 1.5 Å~ 3.0 Å.^{41,42} The binding energy only slightly changes after the atom relaxation except for the HfO₂/As(1) interface. The binding energies for HfO₂/Ga(2) and SrO/Ga(1) are still lower than those for other interface configurations.

The atoms near interface will migrate after atom relaxation. The positive value indicates that the atom moves toward the interface, while the negative value indicates that the atom moves away from the interface. The results show that O has a larger migration on HfO₂ layer than on SrO layer. Hf has smaller migration than Sr. The migration of Ga and As is less than 0.1 Å. The charge in Table 2 represents the charge transfer from GaAs slab to SrHfO₃ slab, which is the number of extra electrons on SrHfO₃ slab. The interface characteristics can be investigated by the analysis of charge transfer.⁴³ It is noted that HfO₂ layer is easier to get electrons than SrO layer. This may be due to the fact that HfO₂ layer has more oxygen atoms than SrO layer. The charge is -0.70 e for HfO₂/Ga(1), -1.08 e for HfO₂/Ga(2), -0.72 e for HfO₂/Ga(3), -0.40 e for SrO/Ga(1), and -0.08 e for SrO/Ga(2). Because electronegativity of As is greater than that of Ga, the charge transfers at HfO₂/As and SrO/As interfaces are smaller than those at HfO₂/Ga and SrO/Ga interfaces. Anomalous charge transfer is observed for SrO/As(1) and SrO/As(2) interfaces. The charge is 0.17 e for SrO/As(1), 0.20 e for SrO/As(2), which suggests that As obtains electrons from SrO layer.

In the potential alignment method, the valence band offset (VBO) is determined by two terms.^{11,44}

$$\text{VBO} = \Delta E_v + \Delta V \quad (3)$$

The first contribution of ΔE_v corresponds to alignment of valence band maximum (VBM) for bulk band structure term. The second term of ΔV corresponds to the macroscopic averaged electrostatic potential (AEP) alignment. Because of the error between the calculated and experimental band gap, we can't get the exact CBO by calculated band gap. In this study, we obtain CBO by the relation $\text{CBO} = \text{VBO} + E_g^{\text{SrHfO}_3(\text{EXP})} - E_g^{\text{GaAs}(\text{EXP})}$.³⁹ Table 2 shows that the VBO and CBO are closely related to the interface configurations, which is in agreement with previous investigation.⁴⁵⁻⁴⁸ The VBO and CBO are determined to be 2.89 eV and 1.70 eV for HfO₂/Ga(1), 4.40 eV and 0.19 eV for HfO₂/Ga(2), 3.57

eV and 1.02 eV for $\text{HfO}_2/\text{Ga}(3)$, 4.38 eV and 0.21 eV for $\text{SrO}/\text{Ga}(1)$, 2.91 eV and 1.68 eV for $\text{SrO}/\text{Ga}(2)$, 2.50 eV and 2.09 eV for $\text{HfO}_2/\text{As}(1)$, 2.81 eV and 1.78 eV for $\text{HfO}_2/\text{As}(2)$, 3.04 eV and 1.55 eV for $\text{HfO}_2/\text{As}(3)$, 2.12 eV and 2.76 eV for $\text{SrO}/\text{As}(1)$, 1.92 eV and 2.67 eV for $\text{SrO}/\text{As}(2)$. The VBO and CBO for ideal MOS devices should be larger than 1 eV, which can effectively prevent leakage current. Previous investigation showed that the VBO and CBO are 2.66 eV and 1.33 eV for ZrO_2/GaAs .⁴⁹ Yang et al. found that VBO for $\text{La}_2\text{O}_3/\text{GaAs}$ interface is about 1.7 eV.⁵⁰ Jin et al. found that the experimental VBO changes from 2.86 eV to 3.36 eV when the annealing temperature increases from 600 °C to 800 °C.⁵¹

In this study, we do not consider the effect of interface defects. Defects inevitably exist in the actual interface. Previously, Alay-e-Abbas et al. investigated formation energies of vacancy defect in SrHfO_3 .⁵² The results show that ordered oxygen vacancies in HfO_2 layer are energetically favorable. Chen et al did a systematic study of stability diagram and electronic properties for (110) SrHfO_3 polar terminations.⁵³ They found that the atomic defect on the surface layer dominates the stabilization for SrHfO_3 . We believe that the defects near $\text{SrHfO}_3/\text{GaAs}$ interface will affect the band offset, which should be further studied.

B. Interface properties of $\text{HfO}_2/\text{Ga}(2)$ and $\text{SrO}/\text{Ga}(1)$ configurations

Figure 4 presents a schematic representation of the band alignment for $\text{HfO}_2/\text{Ga}(2)$ and $\text{SrO}/\text{Ga}(1)$. The planar and macroscopic AEP are presented in Fig. 4. The planar AEP in the atomic region shows periodic oscillations, while it keeps constant in the vacuum region (see blue curve), which is in agreement with previous investigation.^{3,4,54} In order to accurately calculate band offsets, we have to eliminate the interface polarization effect. The polarization inside SrHfO_3 and GaAs can be avoided by a symmetric slab. During calculations, the dipole correction is also applied to remove the possible interface polarization induced by charge transfer between the oxide and semiconductor. For $\text{HfO}_2/\text{Ga}(2)$, macroscopic AEP value is -12.14 eV for SrHfO_3 and -7.31 eV for GaAs . E_v (valence band maximum) and E_c (conduction band minimum) are -6.55 eV and -0.54 eV for SrHfO_3 and -2.17 eV and -0.75 eV for GaAs . For $\text{SrO}/\text{Ga}(1)$ interface, the value of macroscopic AEP is -14.85 eV for SrHfO_3 and -10.00 eV for GaAs . E_v and E_c are -9.26 eV and -3.25 eV for SrHfO_3 and -4.86 eV and -3.44 eV for GaAs . The VBO and CBO for $\text{HfO}_2/\text{Ga}(2)$ and $\text{SrO}/\text{Ga}(1)$ are also shown in Fig. 4.

We investigate the VBO and charge transfer versus interface spacing for $\text{HfO}_2/\text{Ga}(2)$ and $\text{SrO}/\text{Ga}(1)$ interfaces, which is shown in Fig. 5. For $\text{HfO}_2/\text{Ga}(2)$ interface, VBO keeps small change as interface spacing is in the range from 2.1 Å to 2.8 Å. This reflects strong

interaction between SrHfO_3 and GaAs . VBO decreases as the interface spacing is in the range from 2.8 Å to 3.2 Å, which corresponds to the weakening interface interaction. The result can also be verified by the charge transfer. It is found that the charge on SrHfO_3 slab decreases with the increase of the interface spacing. The charge changes from -1.08 e to -0.60 e as the interface spacing increases from 2.1 Å to 3.2 Å. Similar behavior is also found on $\text{SrO}/\text{Ga}(1)$. Comparing with $\text{HfO}_2/\text{Ga}(2)$, the charge transfer at $\text{SrO}/\text{Ga}(1)$ is small. It is noted that the interface spacing affects the band offsets, resulting in deviation between theoretical calculation and experiment.^{55–58}

The layer electronic density of states for $\text{SrO}/\text{Ga}(1)$ and $\text{HfO}_2/\text{Ga}(2)$ is presented in Fig.6. The chemical formula of symmetric slab is $\text{Hf}_{20}\text{Sr}_{24}\text{O}_{64}/\text{Ga}_{36}\text{As}_{32}$ for $\text{SrO}/\text{Ga}(1)$ and $\text{Hf}_{24}\text{Sr}_{20}\text{O}_{68}/\text{Ga}_{36}\text{As}_{32}$ for $\text{HfO}_2/\text{Ga}(2)$. In order to elucidate the effect of the polarization on the interfacial properties, we also investigate $\text{SrHfO}_3/\text{GaAs}$ interface with ideal stoichiometry. The chemical formula is $\text{Hf}_{20}\text{Sr}_{20}\text{O}_{60}/\text{Ga}_{32}\text{As}_{32}$ for $\text{SrO}/\text{Ga}(1)$ and $\text{HfO}_2/\text{Ga}(2)$ configurations, which is also called as unsymmetric slab. It is found that $\text{SrO}/\text{Ga}(1)$ and $\text{HfO}_2/\text{Ga}(2)$ exhibit metallic behavior, which is in agreement with previous investigation.²¹ The metallic behavior for $\text{HfO}_2/\text{Ga}(2)$ and $\text{SrO}/\text{Ga}(1)$ occurs only on several atom layers near the interface. The polarization inside SrHfO_3 and GaAs does not affect the interface behavior. The gap states in SrHfO_3 are mainly determined by Hf 5d, Sr 4d, O 2p. The gap states in GaAs is dominated by Ga 4s, 4p and As 4s, 4p. We believe that the metal interface is mainly caused by the interfacial charge transfer, which will lead to carrier tunneling and increasing the leakage current of the electronic devices.^{59,60} Previously, wang et al. explained that the metallicity in $\text{SrHfO}_3/\text{GaAs}$ interface originates from the surface electron accumulation.²¹ Alay-e-Abbas et al found that the metal behavior in SrHfO_3 is due to charge transfer between vacancy site and the hafnium dangling bond.⁵² In order to eliminate the metal interface, the electrons near the interface should form stable covalent bonds. The interface issues still need to be further studied.

To further understand the bonding, the electron density difference of $\text{SrO}/\text{Ga}(1)$ is given in Fig. 7. The charge density is mainly distributed around O, while Sr and Hf have almost no charge density. In GaAs slab, the charge density is mainly distributed between Ga and As. Because As has a greater electronegativity than Ga, the charge density is slightly closer to As. This result strongly suggests that the ionic bond is formed between O and Sr (Hf), while polar covalent bond is formed between Ga and As. We also test the effect of polar SrHfO_3 and GaAs slabs on electron density. We can find no significant change in electron density using polar SrHfO_3 and GaAs slabs. Similar behavior is also found at $\text{HfO}_2/\text{Ga}(2)$ interface. This analysis is consistent with previous investigations.^{61–63} The charge transfers for $\text{SrO}/\text{Ga}(1)$ and $\text{HfO}_2/\text{Ga}(2)$ interfaces occur

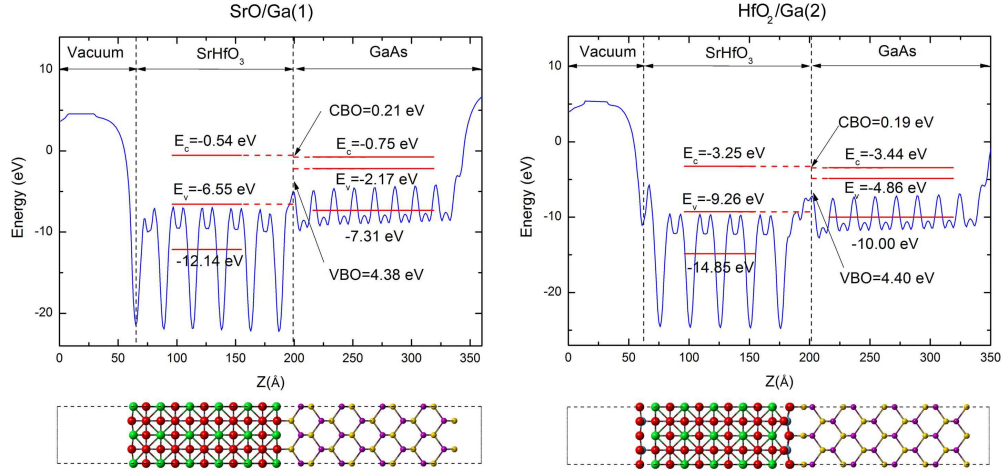


FIG. 4. Schematic representation of the band alignment for SrO/Ga(1) and HfO₂/Ga(2) configurations (top panel). Blue curve denotes planar averaged electrostatic potential (AEP). Macroscopic AEP, valence band maximum (E_v), conduction band minimum (E_c), band offsets (VBO and CBO) are also presented in figure. A schematic view of the SrHfO₃/GaAs interface is shown in the bottom panel. The Sr, Hf, O, Ga and As atoms are marked by large green, large blue, large red, small yellow and small violet spheres, respectively.

mainly between interfacial O and Ga. O near interface will obtain more electrons than those in bulk SrHfO₃, while Ga near interface will lose more electrons than those in bulk GaAs. The interaction between interfacial O and Ga should be a typical ionic bond.

IV. CONCLUSIONS

Geometry structures and electronic properties of SrHfO₃/GaAs interface are investigated by density functional theory (DFT). O is more favorable for adsorption on Ga surface than on As surface. Ten possible interface configurations on SrHfO₃/GaAs interface are investigated. The results show that the band offsets, interface spacing, binding energy and charge transfer are different for ten configurations. The interface spacing is in the range from 1.7 Å to 2.9 Å, and the charge transfer is in the range from 0.20 e to -1.08 e. Both HfO₂/Ga(2) and SrO/Ga(1) interfaces are lower in binding energy than other interface configurations, which suggests that they have a stable structure. Electronic density of states for HfO₂/Ga(2) and SrO/Ga(1) suggests that they exhibit metallic interface behavior. The charge transfer occurs mainly from interfacial Ga to O, which suggests that the interaction between interfacial O and Ga is typical ionic bond. As the interface spacing increases, VBO begins to undergo small changes and then monotonically decreases. We also find that the charge transfer decreases with the increase of interface spacing, which corresponds to the weakening interface interaction.

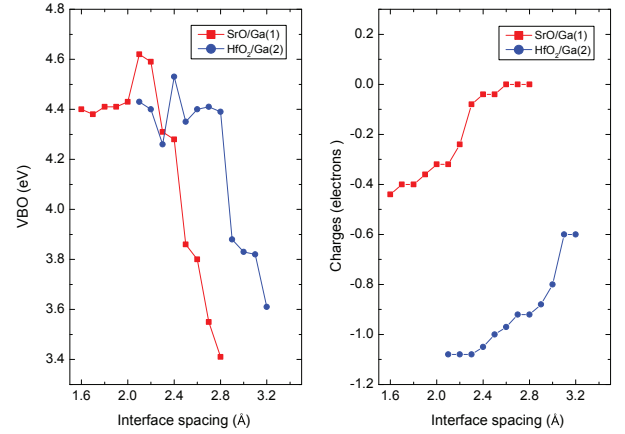


FIG. 5. VBO and charges versus interface spacing for SrO/Ga(1) and HfO₂/Ga(2) configurations.

ACKNOWLEDGMENTS

The work is supported by the Science Foundation from Education Department of Liaoning Province, China (Grant Nos. LF2017001 and LQ2017005).

REFERENCES

- ¹G. He, L. Zhu, Z. Sun, Q. Wan, and L. Zhang, Progress in Materials Science **56**, 475 (2011).

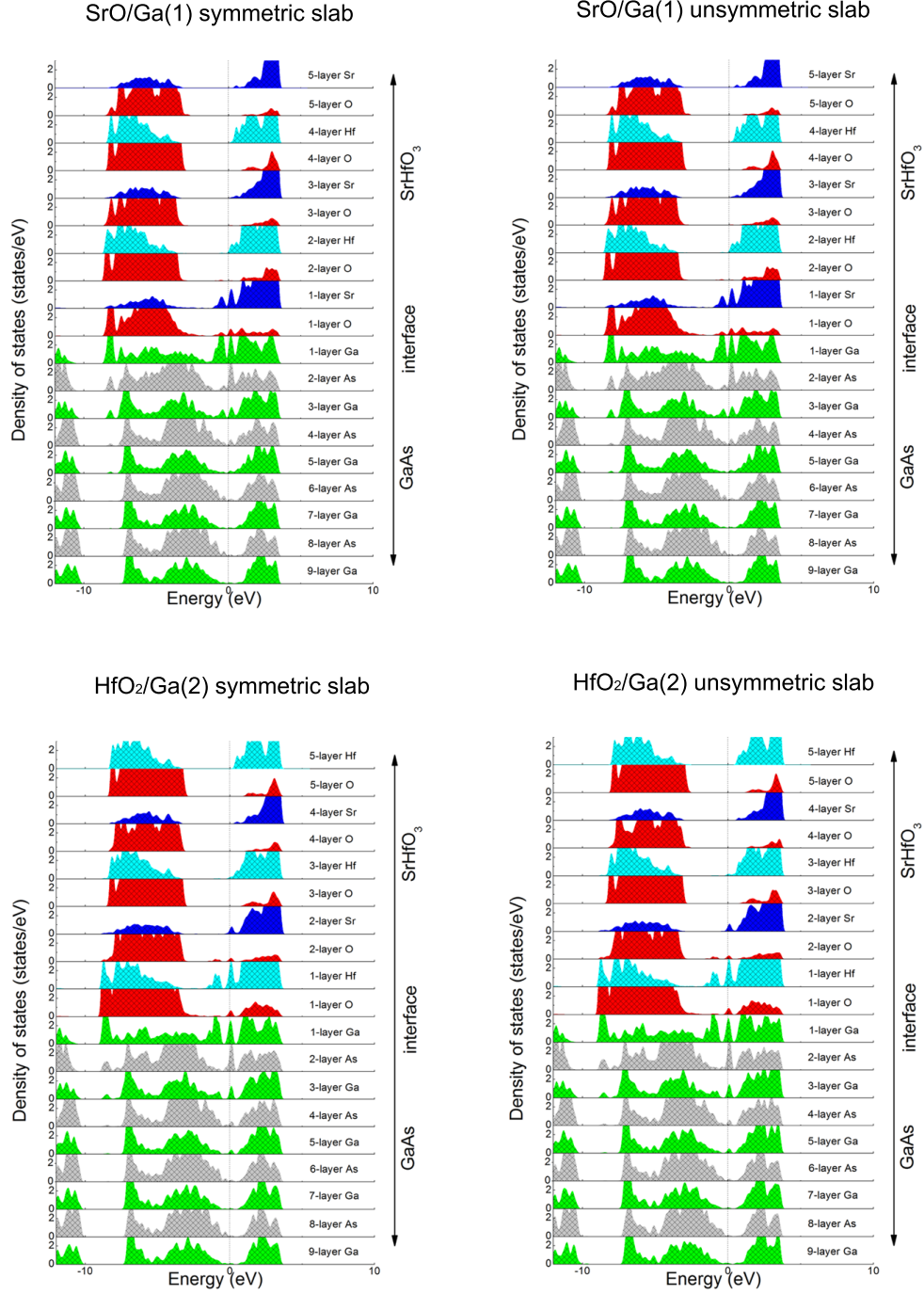


FIG. 6. Density of states of (001) $\text{SrHfO}_3/\text{GaAs}$ interfaces. The layer density of states for $\text{SrO}/\text{Ga}(1)$ and $\text{HfO}_2/\text{Ga}(2)$ configurations is presented. The vertical dotted line denotes Fermi level. The symmetric and unsymmetric slabs are considered.

²D. Y. Cho, H. S. Jung, and C. S. Hwang, Physical Review B **82**, 094104 (2010).

³M. Yang, R. Wu, W. Deng, L. Shen, Z. Sha, Y. Cai, Y. Feng, and S. Wang, Journal of Applied Physics **105**, 024108 (2009).

⁴M. Yang, G. Peng, R. Wu, W. Deng, L. Shen, Q. Chen, Y. Feng, J. Chai, J. Pan, and S. Wang, Applied Physics Letters **93**, 222907 (2008).

⁵M. Hong, J. Kwo, A. Kortan, J. Mannaerts, and A. Sergent, Science **283**, 1897 (1999).

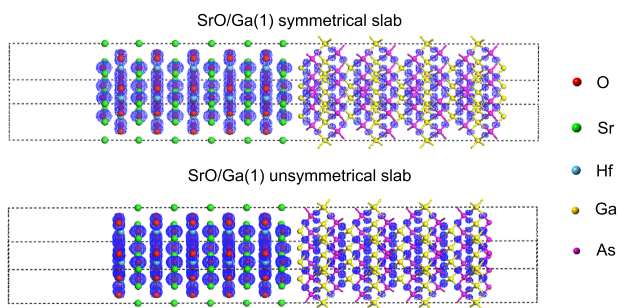


FIG. 7. The electron density difference for SrO/Ga(1) configuration with symmetrical and unsymmetrical slabs.

- ⁶F. C. Chiu, H. W. Chou, and J. Y. Lee, *Journal of Applied Physics* **97**, 103503 (2005).
- ⁷S. Wu, K. Chen, Y. Lin, C. Cheng, C. Hsu, J. Kwo, and M. Hong, *Microelectronic Engineering* **147**, 310 (2015).
- ⁸M. Choi, J. L. Lyons, A. Janotti, and C. G. V. De Walle, *Applied Physics Letters* **102**, 142902 (2013).
- ⁹J. X. Zheng, G. Ceder, T. Maxisch, W. K. Chim, and W. K. Choi, *Physical Review B* **75**, 104112 (2007).
- ¹⁰J. Kang, E. Lee, and K. J. Chang, *Physical Review B* **68**, 054106 (2003).
- ¹¹N. R. D'Amico, G. Cantele, and D. Ninno, *Applied Physics Letters* **101**, 141606 (2012).
- ¹²L. Feng, R. Jia, and Z. Liu, *Rare Metal Materials and Engineering* **43**, 2619 (2014).
- ¹³Q.-J. Liu, Z.-T. Liu, L.-P. Feng, and H. Tian, *Physica B: Condensed Matter* **407**, 2239 (2012).
- ¹⁴Q.-J. Liu, Z.-T. Liu, J.-C. Chen, L.-P. Feng, H. Tian, and W. Zeng, *Applied Surface Science* **258**, 3455 (2012).
- ¹⁵M. Sawkar-Mathur, C. Marchiori, J. Fompeyrine, M. F. Toney, J. Bargar, and J. P. Chang, *Thin Solid Films* **518**, S118 (2010).
- ¹⁶G. He, X. Chen, and Z. Sun, *Surface Science Reports* **68**, 68 (2013).
- ¹⁷M. D. McDaniel, C. Hu, S. Lu, T. Q. Ngo, A. Posadas, A. Jiang, D. J. Smith, E. T. Yu, A. A. Demkov, and J. G. Ekerdt, *Journal of Applied Physics* **117**, 054101 (2015).
- ¹⁸M. Sousa, C. Rossel, C. Marchiori, H. Siegwart, D. Caimi, J.-P. Locquet, D. Webb, R. Germann, J. Fompeyrine, K. Babich, *et al.*, *Journal of Applied Physics* **102**, 104103 (2007).
- ¹⁹M. Sawkar-Mathur, C. Marchiori, J. Fompeyrine, M. F. Toney, J. Bargar, and J. P. Chang, *Thin Solid Films* **518**, S118 (2010).
- ²⁰D. Rai, A. Shankar, A. P. Sakhya, T. Sinha, B. Merabet, R. Khenata, A. Bouchani, S. Solaymani, R. Thapa, *et al.*, *Materials Chemistry and Physics* **186**, 620 (2017).
- ²¹J. Wang, M. Yuan, G. Tang, H. Li, J. Zhang, and S. Guo, *Journal of Applied Physics* **119**, 235304 (2016).
- ²²R. Konda, C. White, J. Smak, R. Mundle, M. Bahoura, and A. Pradhan, *Chemical Physics Letters* **583**, 74 (2013).
- ²³H.-L. Lu, M. Yang, Z.-Y. Xie, Y. Geng, Y. Zhang, P.-F. Wang, Q.-Q. Sun, S.-J. Ding, and D. Wei Zhang, *Applied Physics Letters* **104**, 161602 (2014).
- ²⁴H. J. Monkhorst and J. D. Pack, *Physical Review B* **13**, 5188 (1976).
- ²⁵J. Heyd, G. E. Scuseria, and M. Ernzerhof, *The Journal of Chemical Physics* **118**, 8207 (2003).
- ²⁶J. Heyd and G. E. Scuseria, *The Journal of Chemical Physics* **121**, 1187 (2004).
- ²⁷J. Paier, M. Marsman, K. Hummer, G. Kresse, I. Gerber, and J. Ángyán, *Journal of Chemical Physics* **125**, 249901 (2006).
- ²⁸J. Heyd, J. E. Peralta, G. E. Scuseria, and R. L. Martin, *The Journal of Chemical Physics* **123**, 174101 (2005).
- ²⁹L. B. Shi, M. B. Li, X. M. Xiu, X. Y. Liu, K. C. Zhang, Y. H. Liu, C. R. Li, and H. K. Dong, *Journal of Applied Physics* **121**, 205305 (2017).
- ³⁰T. Windhorn, L. Cook, and G. Stillman, *IEEE Electron Device Letters* **3**, 18 (1982).
- ³¹B. Stankiewicz and P. Mikolajczyk, *Applied Surface Science* **384**, 263 (2016).
- ³²W. Ji, Z. Shen, M. Fan, P. Su, Q. Tang, and C. Zou, *Chemical Engineering Journal* **283**, 58 (2016).
- ³³D. Li, H. Luo, J. Cai, Y. Cheng, X. Shao, and C. Dong, *Applied Surface Science* **403**, 645 (2017).
- ³⁴A. V. Bakulin, S. E. Kulkova, M. S. Aksenov, and N. A. Valisheva, *The Journal of Physical Chemistry C* **120**, 17491 (2016).
- ³⁵S. Mallik, S. Mallick, and S. Bedanta, *Journal of Magnetism and Magnetic Materials* **428**, 50 (2017).
- ³⁶J. Kacher, K. Hattar, and I. M. Robertson, *Materials Science and Engineering: A* **675**, 110 (2016).
- ³⁷W.-B. Zhang, C. Chen, and P.-Y. Tang, *The Journal of Chemical Physics* **141**, 044708 (2014).
- ³⁸K. Yao, H. Huang, and Z. Liu, *Physica B: Condensed Matter* **403**, 3191 (2008).
- ³⁹Y.-W. Cheng, F.-L. Tang, H.-T. Xue, H.-X. Liu, B. Gao, and Y.-D. Feng, *Journal of Physics D: Applied Physics* **49**, 285107 (2016).
- ⁴⁰K. Li, Z. Sun, F. Wang, N. Zhou, and X. Hu, *Applied Surface Science* **270**, 584 (2013).
- ⁴¹X. M. He, Z. M. Chen, L. Huang, and L. B. Li, *Modern Physics Letters B* **29**, 1550182 (2015).
- ⁴²K. Luo, Q. Deng, X. Zha, Q. Huang, J. S. Francisco, X. Yu, Y. Qiao, J. He, and S. Du, *Molecular Physics* **113**, 1 (2015).
- ⁴³M. Stefan, D. Toloman, A. Popa, A. Mesaros, O. R. Vasile, C. Leostean, and O. Pana, *Journal of Nanoparticle Research* **18**, 1 (2016).
- ⁴⁴L. Silvestri, J. Cervenka, S. Praver, and F. Ladouceur, *Diamond and Related Materials* **31**, 25 (2013).
- ⁴⁵X. Zhang, A. Demkov, H. Li, X. Hu, Y. Wei, and J. Kulik, *Physical Review B* **68**, 125323 (2003).

- ⁴⁶C. Hajlaoui, L. Pedesseau, F. Raouafi, F. B. C. Larbi, J. Even, and J.-M. Jancu, *Journal of Physics D: Applied Physics* **48**, 355105 (2015).
- ⁴⁷Y. Dong, Y. Feng, S. Wang, and A. Huan, *Physical Review B* **72**, 045327 (2005).
- ⁴⁸W. Bao and M. Ichimura, *Japanese Journal of Applied Physics* **52**, 061203 (2013).
- ⁴⁹Y.-P. Wang, Y.-P. Wang, and L.-B. Shi, *Chinese Physics Letters* **32**, 016102 (2015).
- ⁵⁰J. Yang and H. Park, *Applied Physics Letters* **87**, 202102 (2005).
- ⁵¹H. Jin, S. K. Oh, and H. J. Kang, *Journal of Surface Analysis* **12**, 254 (2005).
- ⁵²S. M. Alay-e-Abbas, S. Nazir, N. A. Noor, N. Amin, and A. Shaukat, *The Journal of Physical Chemistry C* **118**, 19625 (2014).
- ⁵³H. Chen, H. T. Yu, and Y. Xie, *Materials Chemistry and Physics* **174**, 195 (2016).
- ⁵⁴M. Yang, J. W. Chai, M. Callsen, J. Zhou, T. Yang, T. T. Song, J. S. Pan, D. Z. Chi, Y. P. Feng, and S. J. Wang, *The Journal of Physical Chemistry C* **120**, 9804 (2016).
- ⁵⁵J. Tao, J. W. Chai, Z. Zhang, J. S. Pan, and S. J. Wang, *Applied Physics Letters* **104**, 232110 (2014).
- ⁵⁶L. B. Shi, M. B. Li, X. M. Xiu, X. Y. Liu, K. C. Zhang, C. R. Li, and H. K. Dong, *Physica B* **510**, 13 (2017).
- ⁵⁷L. B. Shi, X. Y. Liu, and H. K. Dong, *Journal of Applied Physics* **120**, 105306 (2016).
- ⁵⁸Y. Li, Y. Li, J. Wang, Z. He, Y. Zhang, Q. Yu, and J. Hou, *Journal of Electron Spectroscopy and Related Phenomena* **217**, 1 (2017).
- ⁵⁹C. Y. Chang, O. Ichikawa, T. Osada, M. Hata, H. Yamada, M. Takenaka, and S. Takagi, *Journal of Applied Physics* **118**, 085309 (2015).
- ⁶⁰Y. C. Yeo, Q. Lu, W. C. Lee, T.-J. King, C. Hu, X. Wang, X. Guo, and T. Ma, *IEEE Electron Device Letters* **21**, 540 (2000).
- ⁶¹W. Sun, L. Zhang, J. Liu, H. Wang, and Y. Bu, *Computational Materials Science* **111**, 175 (2016).
- ⁶²Y. Liu, J. Xing, Y. Li, L. Sun, and Y. Wang, *Applied Surface Science* **405**, 497 (2017).
- ⁶³Y. Xian, R. Qiu, X. Wang, and P. Zhang, *Journal of Nuclear Materials* **478**, 227 (2016).